19951/19501

N95-25921

44634

P 9

APPENDIX I

Fragmentation Cross Sections of ^{16}O Between 0.9 and 200 GeV/Nucleon

by

S.E. Hirzebruch, W. Heinrich, K.D. Tolstov, A.D. Kovalenko and E.V. Benton

Fragmentation cross sections of ^{16}O between 0.9 and 200 GeV/nucleon

S. E. Hirzebruch,[1] W. Heinrich,[1] K. D. Tolstov,[2] A. D. Kovalenko,[2] and E. V. Benton[3]
[1]*University of Siegen, Department of Physics, Adolf-Reichweinstr. 2, 5900 Siegen, Germany*
[2]*Laboratory of High Energies, Joint Institute for Nuclear Research, Dubna, Russia*
[3]*University of San Francisco, Department of Physics, San Francisco, California 94177* *
(Received 10 April 1992)

Inclusive cross sections for high energy interactions at 0.9, 2.3, 3.6, and 13.5 GeV/nucleon of ^{16}O with C, CR-39 ($C_{12}H_{18}O_7$), CH_2, Al, Cu, Ag, and Pb targets were measured. The total charge-changing cross sections and partial charge-changing cross sections for the production of fragments with charge $Z=6$ and $Z=7$ are compared to previous experiments at 60 and 200 GeV/nucleon. The contributions of Coulomb dissociation to the total cross sections are calculated. Using factorization rules the partial electromagnetic cross sections are separated from the nuclear components. Energy dependence of both components are investigated and discussed.

PACS number(s): 25.75.+r

I. INTRODUCTION

A. General

Depending on the impact parameter between the colliding nuclei, the type of reaction differs. For an impact parameter smaller than the sum of the projectile's and target's radii, the interaction is dominated by the strong force. For impact parameters which are too large for an overlap of target and projectile nuclei, the interaction is purely electromagnetic. For high projectile energies and strong electromagnetic fields (i.e., high-Z targets), the probability increases that this interaction leads to a fragmentation of the projectile or target nucleus. This effect, which is called electromagnetic dissociation (ED), has become the subject of systematic studies over the last years. Several groups report experimental results for the measurement of ED for different projectile [1–13] and target [14–17] fragmentation reactions. Recently, Olson *et al.* [18] reported direct observation of the giant dipole resonance of ^{16}O via electromagnetic dissociation.

During the last years, we have been measuring fragmentation cross sections for high-energy heavy-ion reactions. In this paper we present our results for ^{16}O projectiles at beam energies of 0.9 GeV/nucleon for H, CH_2, C, and Pb targets and at 2.3, 3.6, and 13.5 GeV/nucleon for H, CH_2, CR-39, C, Al, Cu, Ag, and Pb targets. Cross sections for the hydrogen target were calculated with the subtraction method using the CH_2/C data. We performed the 13.5-GeV/nucleon (14.5-GeV/c momentum) experiment at the Alternating Gradient Synchrotron (AGS) facility at Brookhaven National Laboratory (BNL). The 0.9-, 2.3-, and 3.6-GeV/nucleon experiments were carried out at the Synchrophasotron in Dubna (Russia).

In combination with the earlier published data for ^{16}O at 60 and 200 GeV/nucleon [9], we are now able to analyze the energy dependence of nuclear and electromagnetic cross sections in the energy range from 1 to 200 GeV/nucleon. Our interest is focused onto the following points: (a) The process of electromagnetic dissociation contributes significantly to the total charge-changing cross sections for heavy targets within the investigated energy range. With the complete set of our ^{16}O data, we are able to determine the energy dependence of the ED contribution of different targets to the total charge-changing cross sections. (b) Cross sections for the hydrogen target are important input data for astrophysical calculations which describe the propagation of cosmic-ray nuclei through interstellar space. The energy dependence of hydrogen partial cross sections, which we have observed beyond 1 GeV/nucleon [19,20], can be analyzed in more detail. (c) The validity of factorization rules for partial elemental cross sections for the heavier targets is tested.

B. Experimental setup

We used stacks of CR-39 ($C_{12}H_{18}O_7$) plastic nuclear track detectors, which were mounted up and downstream of the target. One stack consists typically of five sheets of CR-39. The CR-39 used was produced by American Acrylics and has a unique charge resolution. The detection threshold lies near the energy loss for relativistic boron ($Z=5$) ions. The detectors were etched in 6n NaOH at 70 °C for 36 or 48 h. After this procedure etch cones of relativistic nuclei with charges $Z=5-8$ could be detected. Using the advanced Siegen automatic measuring system, we scanned all detector surfaces, which contained typically 70 000 tracks each (1.4×10^6 objects for 1 target and energy). Further detailed information about the experimental setup and the automatic measuring system can be found in [21,22]. Since etch cones for particles with charge 5 were detected with a reduced efficiency, we could only determine partial cross sections for charges 6 and 7.

C. Nuclear and ED total cross sections

The total nuclear cross section is generally parametrized by overlap formulas, which have the form

*USF portion of this work partially supported by NASA Grant No. NAG9-235, Johnson Space Center, Houston, TX.

$$\sigma_{\text{nuc}}^{\text{tot}}(P,T)=\pi(R_T+R_P-\delta_{PT})^2 , \quad (1)$$

where R_T and R_P are the radii of target and projectile nucleus and δ_{PT} takes into account the drop of the nuclear density in the nucleus sphere. Since none of common cross-section formulas [23–26,38] take the ED effect into account (most of them are not even energy dependent), all of them give constant cross-section values for energies greater than 2 GeV/nucleon. This is expected to be correct for the nuclear component of the cross section because of the concept of limiting fragmentation.

For a theoretical description of the ED effect, Bertulani and Baur [27–29] have derived spectra of virtual photons, which are equivalent to the electromagnetic pulse a projectile suffers while passing a target nucleus (or vice versa). The intensity of the photon-number spectra dN/dE_γ is approximately proportional to $Z_T^2 \ln\gamma/E_\gamma$, where Z_T is the target charge, γ is the Lorentz factor of the projectile in the laboratory frame, and E_γ is the energy of an absorbed photon. The nucleus absorbs the photon by giant resonances, by the quasideuteron effect [30], or by resonances which lie in higher-photon-energy regimes (e.g., Δ resonances). The deexcitation of these excited modes can easily lead to the emission of protons or alpha particles or may even cause a severe destruction of the nucleus [10]. For high energies the relativistic contracted field of the target seen by the passing projectile is nearly a plane wave which contains all photon multipolarities with the same strength. In this case the total charge-changing ED cross section can be calculated by

$$\sigma_{\text{em}}^{\text{tot}}=\int n(E_\gamma)\sigma_\gamma(E_\gamma)dE_\gamma , \quad (2)$$

where $n(E_\gamma)$ is the virtual-photon spectrum and $\sigma_\gamma(E_\gamma)$ is the photonuclear charge-changing cross section for ^{16}O, respectively. This is equivalent to the method used by Weizsäcker [31] and Williams [32].

For smaller projectile energies, the strengths of the different multipolarities differ very much, especially in the photon-energy region of the ^{16}O giant resonance. For that reason electrical dipole ($E1$) absorption has to be distinguished from the electrical quadrupole ($E2$) absorption process. The total charge-changing ED cross section can then be calculated by evaluating (3):

$$\sigma_{\text{em}}^{\text{tot}}=\int [n_{E1}(E_\gamma)\sigma_{\gamma E1}(E_\gamma) + n_{E2}(E_\gamma)\sigma_{\gamma E2}(E_\gamma)]dE_\gamma . \quad (3)$$

Since photonuclear cross sections measured with real photon beams contain all absorption modes, separation of the $E1$ and $E2$ contributions has to be performed using several assumptions. In previous calculations of Norbury [33–35], $E2$ contributions were obtained using a Lorentzian distribution as an approximation of the quadrupole excitation cross section in combination with sum rules and empirical formulas for the position of the resonances. This method may be adequate for heavy nuclei. However, for light nuclei such as ^{16}O, for which the $E2$ photon cross section is fragmented in energy, this procedure is possibly incorrect.

In a recent theoretical paper by Fleischhauer and Scheid [36], (γ,n) and (γ,p) $E2$ cross sections for ^{16}O were calculated. In order to determine the charge-changing ED cross section, we use their cross sections $\sigma_{\gamma E2p}$ to calculate $\sigma_{\gamma E2}$. In addition to the (γ,p) process, the (γ,α) process plays an important role in the $E2$ absorption process. We use experimental data compiled by Fuller [37] to determine the contribution of the α channel to $\sigma_{\gamma E2}$ and estimate $\sigma_{\gamma E2\alpha}$ by multiplying the given experimental (γ,α) cross sections by the ratio of the relevant sum-rule values σ_0 in the photon-energy interval from 9 to 29 MeV [37]:

$$\sigma_{\gamma E2\alpha}=\sigma_{\text{expt}}(\gamma,\alpha)\frac{\sigma_0(E2)}{\sigma_0(E1)+\sigma_0(E2)} =\sigma_{\text{expt}}(\gamma,\alpha)0.176 . \quad (4)$$

The charge-changing $E2$ cross section is then calculated with help of (5):

$$\sigma_{\gamma E2}=\sigma_{\gamma E2p}+\sigma_{\text{expt}}(\gamma,\alpha)0.176 . \quad (5)$$

$\sigma_{\gamma E1}$ is obtained by subtracting $\sigma_{\gamma E2}$ from the experimental cross section $\sigma_{\gamma\text{expt}}$:

$$\sigma_{\gamma E1}=\sigma_{\gamma\text{expt}}-\sigma_{\gamma E2} . \quad (6)$$

The total charge-changing ED cross sections were calculated inserting (5) and (6) into (3) and using the virtual-photon spectra derived from Bertulani and Baur [27]. This method is effectively equivalent to using $n=0.978n_{E1}+0.022n_{E2}$ for the virtual-photon spectra in the whole γ-energy regime of the giant resonance. This effective weighting differs from the weighting of $n=0.96n_{E1}+0.04n_{E2}$, which we have used in [9]. The consequences of the different weighting, however, have a negligible influence on the calculated ED cross sections at CERN energies. At lower energies the calculated ED cross sections are about 3% smaller (Pb target, 2.3 GeV) than those using the method described in [9]. More details about the photonuclear data used can be found in [9].

The only adjustable parameter in our calculation of the total charge-changing ED cross section is b_{min}, which is the minimum impact parameter giving the maximum range of the strong force. For our calculations we used the overlap formula of Lindstrom *et al.* [23], which gives total nuclear cross sections σ_L. This parametrization is a fit to the data obtained with ^{12}C and ^{16}O projectiles at low Bevalac energies and is in good agreement with different experimental data, which we have compiled in [9]. We calculate the minimum impact parameter setting $b_{\text{min}}=(\sigma_L/\pi)^{0.5}$.

To determine the error of our calculation, we consider contributions by the error of the measured photonuclear cross section, the different weighting of the photon spectra, and the selection of b_{min}: (i) The error of the photonuclear data is estimated to be about 6% (after averaging where possible over several experimentalists data) [9]. (ii) Considering the weighting of different multipolarities, we assume an error of 50% for the calculated $E2$ cross section. This leads to a contribution to the total error of $\sigma_{\text{em}}^{\text{tot}}$ of about 4% for 2.3 GeV/nucleon and decreases to 1% at 200 GeV/nucleon. (iii) The influence of b_{min} on

TABLE I. Measured cross sections for ^{16}O projectiles. All cross sections are given in mb.

Target	Total charge-changing cross section	Partial cross section $\Delta Z=1$	Partial cross section $\Delta Z=2$
	0.9 GeV/nucleon		
H	302.6±22.7	67.5±4.8	67.3±5.7
CH_2	500.3±9.6	81.5±1.9	88.3±2.0
C	895.8±35.1	109.3±3.9	130.4±4.7
Pb	3426.0±204.7	277.8±15.1	301.9±15.8
	2.3 GeV/nucleon		
H	307.3±29.4	54.8±4.8	61.0±5.7
CH_2	497.9±17.7	70.5±2.9	81.2±3.4
CR-39	626.2±21.6	81.7±3.0	90.6±3.4
C	871.1±24.7	101.5±3.9	121.1±4.7
Al	1293.3±32.2	121.8±5.0	142.5±5.8
Cu	1955.2±51.9	162.7±8.2	181.5±9.0
Ag	2498.0±83.6	204.3±10.6	216.1±11.3
Pb	3479.4±142.9	320.8±17.4	299.6±18.0
	3.6 GeV/nucleon		
H	286.9±27.9	52.2±4.6	63.4±5.7
CH_2	481.8±16.8	69.2±2.8	82.6±3.5
CR-39	618.3±17.8	81.9±2.8	89.2±3.3
C	863.8±23.9	102.7±3.6	120.5±4.3
Al	1250.3±32.2	125.5±4.7	147.7±5.4
Cu	1941.8±51.9	171.7±9.7	188.4±9.2
Ag	2524.2±70.5	228.1±10.2	203.7±10.3
Pb	3545.8±179.0	389.2±17.1	302.2±19.9
	13.5 GeV/nucleon		
H	284.9±20.0	46.5±4.8	56.3±5.1
CH_2	491.0±12.2	67.7±3.0	75.5±3.2
CR-39	627.9±13.0	80.0±2.6	86.0±2.8
C	895.0±15.3	109.4±3.7	113.4±3.9
Al	1309.0±27.2	143.9±5.1	140.5±5.5
Cu	2042.0±54.0	219.2±9.0	193.9±9.0
Ag	2693.0±66.2	311.5±11.4	225.9±10.2
Pb	3936.0±76.0	588.7±22.3	334.4±17.8

the error of σ_{em}^{tot} is estimated by comparing predictions of empirical cross-section formulas. In addition to the formula of Lindstrom *et al.* [23], we use the parametrizations of Westfall *et al.* [24] and Benesh, Cook, and Vary [38]. Differences in b_{min} reach a maximum for the lead target. We use $\Delta b_{min}/b_{min}=5.7\%$, which is deduced from half the difference of b_{min} determined after Westfall *et al.* [24] and Lindstrom *et al.* [23] for the lead target. The compiled data of [9], which are best described by the formula of Lindstrom *et al.*, lie within the range of this error. The error to σ_{em}^{tot} inferred by the uncertainty of b_{min} is about 4.8% for the lower-energy data (0.9 GeV) and 1% for CERN energy data.

Assuming independence of the error sources, we obtain a total error of σ_{em}^{tot} of 10.3%, 7.6%, 7.5%, 6.6%, 6.2%, and 6.1% for the 0.9-, 2.3-, 3.6-, 13.5-, 60-, and 200-GeV/nucleon data, respectively. A further error source is multiple-photon excitation. Llope and Braun-Munziger [39] have shown that the contribution of multiple-photon excitation for ^{28}Si interacting with a Pb target accounts about 1% to the total ED cross section, almost independent of projectile energy. For the ^{16}O projectile, this effect should be even smaller than for ^{28}Si. According to the calculations of Llope and Braun-Munziger for ^{16}O and ^{238}U target [39], higher-order excitation contributes only 0.83% to the total ED cross section at 100 GeV/nucleon. An effect of this strength can be neglected in our case since the other errors discussed are considerably larger. For other projectile, target, and energy combinations, however, the contribution of multiple-photon excitation can be more significant [39,40].

II. RESULTS

The obtained experimental total and partial cross sections for charges 6 and 7 for the 0.9-, 2.3-, 3.6-, and 13.5-GeV/nucleon experiments are listed in Table I. The cross sections for the hydrogen target were calculated using the cross sections for CH_2 and C targets.

A. Total charge-changing cross sections

The calculated total charge-changing ED cross sections are given in Table II. The determined total ED cross sections were subtracted from the measured total ones to derive the pure nuclear component. In Fig. 1 we show measured total cross sections (solid squares), calculated ED cross sections (solid triangles), and difference cross sections (open squares) for Pb, Ag, and Cu targets. The horizontal lines give the average value of the difference cross section for the five energies (six for the lead target). The nuclear fragmentation cross sections obviously are constant at high energies. This means that the method we use succeeded in estimating the energy dependence of the ED contribution to the total reaction cross section.

The difference cross sections for the light targets H, C, and Al where the ED contribution is small are shown in Fig. 2. For these targets the total charge-changing cross sections are also constant in the whole energy regime from 2.3 to 200 GeV/nucleon.

The averaged nuclear cross sections for the five heavier targets and all energies are compared with results which

TABLE II. Calculated total ED cross sections for ^{16}O. All cross sections are given in mb.

Target	Kinetic energy (GeV/nucleon) 2.3	3.6	13.5	60	200
C	2.0±0.1	2.4±0.2	4.5±0.3	8.3±0.5	12.0±0.7
Al	7.8±0.6	9.7±0.7	19.0±1.3	36.1±2.2	53.6±3.3
Cu	32.7±2.5	41.6±3.1	84.9±5.6	166.8±10.3	251.7±15.4
Ag	76.0±5.8	98.5±7.4	207.4±13.7	416.6±25.8	636.6±38.8
Pb	194.4±14.8	259.4±19.5	573.0±37.8	1184.7±73.5	1841.2±112.3

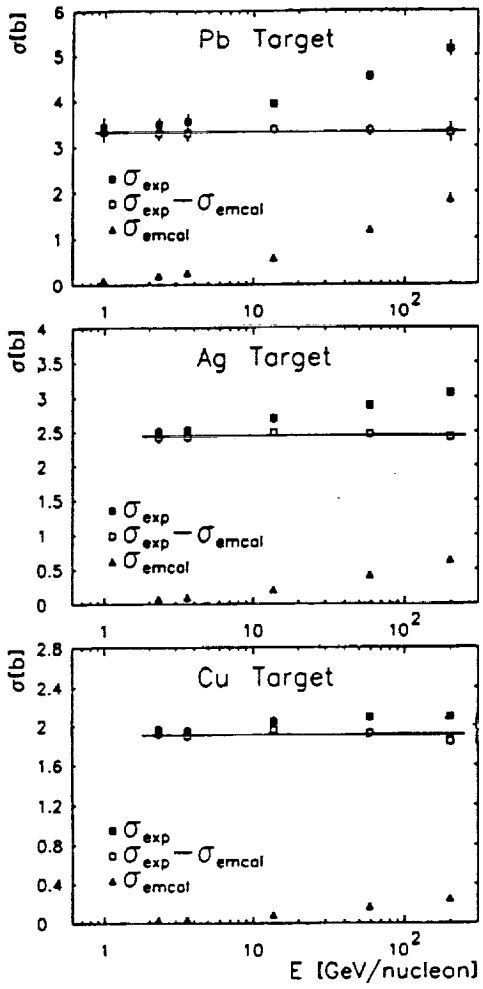

FIG. 1. Energy dependence of ^{16}O charge-changing cross-section data for Pb (top), Ag (middle), and Cu (bottom) targets. The solid squares show the measured reaction cross sections, while the solid triangles represent the calculated charge-changing electromagnetic cross sections. The difference cross sections, which include errors from measured and calculated cross sections, are given by the open squares. The horizontal line represents the average value of difference cross sections for all energies.

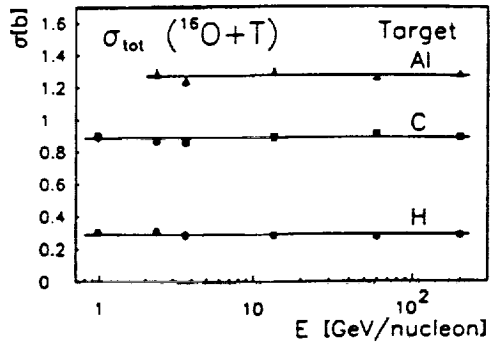

FIG. 2. Energy dependence of ^{16}O cross-section data for the light targets H (results are calculated from C and CH_2 targets), C, and Al after subtraction of the ED component. The horizontal line represents the average value of our cross-section data for all energies.

are obtained from empirical formulas. The empirical estimations of Westfall *et al.* [24] and Binns *et al.* [26] give total charge-changing cross sections as measured in our experiment. The formulas of Lindstrom *et al.* [23], Benesh, Cook, and Vary [38], and Kox *et al.* [25] give the total nuclear reaction cross sections. In order to compare our data with the results of these formulas, we have to estimate the contribution of the σ ($Z=8\rightarrow 8$) neutron-emission channel. This contribution is obtained by using the data of Olson *et al.* [41] from a similar experiment (^{16}O projectile fragmentation at 2.1 GeV/nucleon), which allows the calculation of this contribution with the help of factorization rules. As can be seen in Table III, the measured cross sections agree with the total charge- and mass-changing cross sections derived from different formulas. Only the value for the lead target is overestimated by some formulas. (All formulas are energy independent above 2 GeV/nucleon and do not take into account the ED contribution.)

B. Partial charge-changing cross sections

Partial nuclear cross sections can be described by the factorization rule expressed as

TABLE III. Total nuclear cross sections in comparison to results of different cross section formulas. The first column gives the averaged value of the nuclear cross sections for our experiments at five energies. The next two columns include charge-changing cross sections derived from empirical formulas. In the fourth column, the average total cross sections including the neutron-emission channel are given. The contribution of this channel was estimated using data of Olson *et al.* [41]. These cross sections are compared with the results of four empirical formulas. All cross sections are given in mb.

Target	Average $\Delta Z>0$	Ref. [24] $\Delta Z>0$	Ref. [26] $\Delta Z>0$	Average +Ref. [41] $\Delta A>0$	Ref. [24] $\Delta A>0$	Ref. [23] $\Delta A>0$	Ref. [38] $\Delta A>0$	Ref. [25] $\Delta A>0$
C	883.4±9.7	906.6	999.2	927.2±9.8	924.0	898.3	987.5	999.3
Al	1271.5±11.9	1259.3	1314.4	1326.8±12.1	1314.2	1290.2	1394.6	1438.5
Cu	1908.5±21.1	1853.6	1811.3	1972.5±21.2	1979.5	1861.9	2054.3	2125.0
Ag	2444.6±31.0	2383.5	2234.0	2515.8±31.2	2577.7	2367.9	2629.1	2699.1
Pb	3313.9±69.7	3311.7	2949.2	3393.0±69.8	3632.9	3249.0	3620.1	3649.2

TABLE IV. Calculated γ_{PT} and ε_{PT} for ^{16}O. For definitions, see text.

Target		Kinetic energy (GeV/nucleon) 2.3	3.6	13.5	60	200
C	γ_{PT}	1.000	1.000	1.000	1.000	1.000
	ε_{PT}	1.000	1.000	1.000	1.000	1.000
Al	γ_{PT}	1.216	1.200	1.204	1.179	1.200
	ε_{PT}	3.980	4.071	4.237	4.372	4.444
Cu	γ_{PT}	1.487	1.485	1.482	1.455	1.439
	ε_{PT}	16.604	17.414	18.944	20.192	20.905
Ag	γ_{PT}	1.669	1.678	1.671	1.648	1.652
	ε_{PT}	38.553	41.213	46.301	50.437	52.871
Pb	γ_{PT}	1.944	1.953	1.943	1.919	1.925
	ε_{PT}	98.660	108.548	127.893	143.427	152.925

$$\sigma_{\text{nuc}}(P,T,F)=\gamma_{PT}\gamma_P^F , \tag{7}$$

where $\sigma_{\text{nuc}}(P,T,F)$ is the nuclear fragmentation cross section for the projectile P incident upon the target T producing the fragment F. The factor γ_P^F depends only on the species of projectile and fragment, while γ_{PT} depends only on the species of projectile and target [41].

We found that in a similar way it is also possible to determine partial electromagnetic cross sections [10]. The photon spectra for different targets at constant beam energies do not change significantly in shape, but only in intensity. Therefore the relative probabilities for the production of different projectile fragments in interactions with different targets should be independent of the target. We introduce a factor ε_P^F, which is proportional to the probability to produce a fragment F by ED in a collision of projectile P with an arbitrary target. At a given energy, the absolute value of the partial ED cross section into a given channel is expected to scale with the intensities of the photon spectra associated with each target. We use the target factors γ_{PT} and ε_{PT}, defined separately for each energy as

$$\gamma_{PT}:=\sqrt{\sigma_{\text{nuc}}(P,T)/\sigma_{\text{nuc}}(P,T=C)} \tag{8}$$

and

$$\varepsilon_{PT}:=\sigma_{\text{emc}}^{\text{tot}}(P,T)/\sigma_{\text{emc}}^{\text{tot}}(P,T=C) , \tag{9}$$

where $\sigma_{\text{nuc}}(P,T)$ is the total nuclear cross section for the target T obtained by subtracting the calculated total charge-changing ED cross sections $\sigma_{\text{emc}}^{\text{tot}}(P,T)$ from the measured data. The scaling on the C target is arbitrary, and so scaling to a different target does not lead to any difference in the separated cross sections.

The partial ED cross section is written as

$$\sigma_{\text{em}}(P,T,F)=\varepsilon_{PT}\varepsilon_P^F . \tag{10}$$

For the measured partial cross sections $\sigma_{\text{meas}}(P,T,F)$, we can write

$$\sigma_{\text{meas}}(P,T,F)=\gamma_{PT}\gamma_P^F+\varepsilon_{PT}\varepsilon_P^F . \tag{11}$$

The fragment factors γ_P^F and ε_P^F are evaluated for all energies and fragments by minimizing the expression

$$\sum_T \frac{[\gamma_{PT}\gamma_P^F+\varepsilon_{PT}\varepsilon_P^F-\sigma_{\text{meas}}(P,T,F)]^2}{[\Delta\sigma_{\text{meas}}(P,T,F)]^2} \rightarrow \text{minimum} , \tag{12}$$

where $\Delta\sigma_{\text{meas}}(P,T,F)$ is the error of the measured partial cross section $\sigma_{\text{meas}}(P,T,F)$.

Nuclear and electromagnetic target factors determined by this procedure are given in Table IV for all five energies. The fragment factors determined by our fit procedure are shown in Table V. Using (7) and (10), the pure nuclear and pure electromagnetic components were determined. In Fig. 3 the partial charge-changing nuclear cross sections $\Delta Z=1$ and 2 are shown together with data of Olson *et al.* at 2.1 GeV/nucleon [41]. In general, our partial nuclear cross sections are constant in the whole energy range and agree with the data of Olson *et al.* It should be noted that all cross sections belong to one fixed energy scale with one fragment factor and its error. For that reason all cross sections for a certain energy but different targets are smaller or bigger than the average for all energies (for example, the 13.5-GeV/nucleon data for $\Delta Z=1$ are significantly larger than the average).

Figure 4 shows the energy dependence of the partial electromagnetic cross sections for the lead target. The cross section $\sigma(Z=8\rightarrow Z\leq 5)$ was calculated by sub-

TABLE V. γ_P^F and ε_P^F as determined from fit procedures. All data are in mb.

	Kinetic energy (GeV/nucleon) 2.3	3.6	13.5	60	200
$\gamma_P^F(Z=7)$	97.50±2.79	99.02±2.65	107.76±2.76	105.01±2.99	105.94±3.96
$\varepsilon_P^F(Z=7)$	1.24±0.17	1.70±0.15	2.94±0.16	5.44±0.21	6.75±0.27
$\gamma_P^F(Z=6)$	116.89±3.25	119.72±3.06	113.72±2.86	122.28±3.16	124.75±4.26
$\varepsilon_P^F(Z=6)$	0.66±0.19	0.45±0.18	0.88±0.14	1.62±0.20	1.98±0.26

144

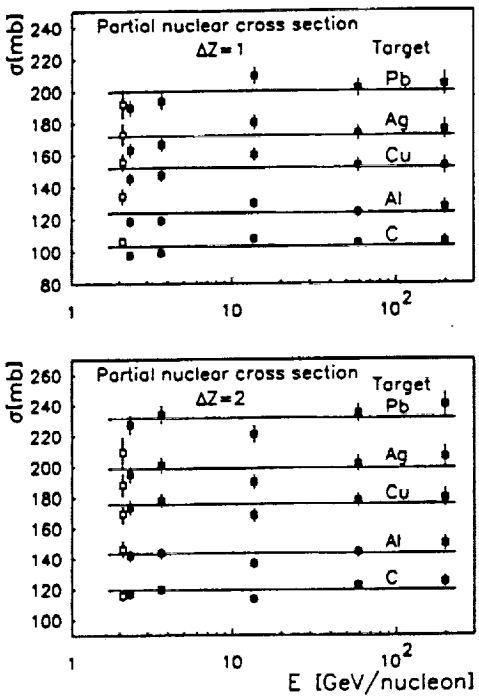

FIG. 3. Partial nuclear cross sections $\Delta Z=1$ (top) and $\Delta Z=2$ (bottom) for the reaction of ^{16}O with targets C, Al, Cu, Ag, and Pb determined from our experiments (solid squares) based on factorization rules. The data include cross sections from [41] at 2.1 GeV/nucleon (open squares). The horizontal line represents the average value of our cross-section data for all energies.

tracting the two partial ED cross sections from the calculated total one. The relative abundance of the ED partial cross sections to the total ED cross sections derived from the data for all targets is shown in Fig. 5. From both figures it can be seen that the partial cross sections for $\Delta Z=1$ and 2 are the dominant electromagnetic interac-

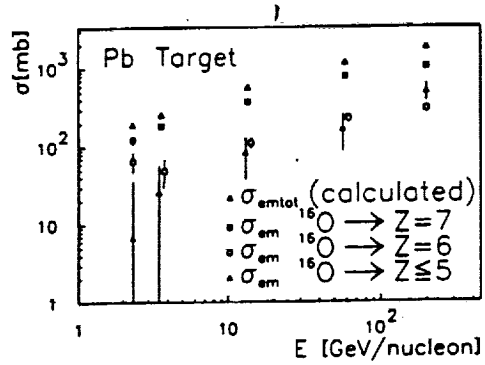

FIG. 4. Partial electromagnetic cross sections for the reaction of ^{16}O with a Pb target. The open triangles give the calculated total charge-changing cross sections. The solid and open squares represent the cross sections for $\Delta Z=1$ and 2, respectively. The solid triangles give the cross section for $\Delta Z\geq 3$, which was calculated by subtracting the $\Delta Z=1$ and 2 contributions from the calculated total ED cross section. Some of the partial cross sections have a small offset in energy for better comparability of the error bars.

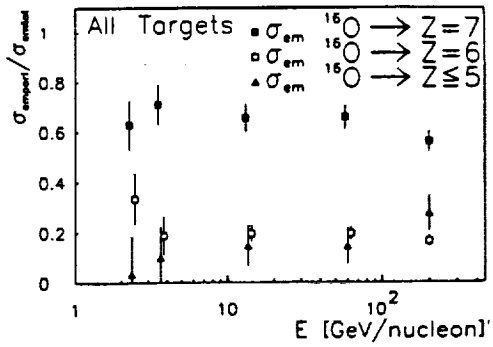

FIG. 5. Relative contributions of partial electromagnetic cross sections for ^{16}O to the total charge-changing electromagnetic cross section. The plot includes results of all targets since the given quotient for one energy only scales with the constant factor ε_p^F. Some of the partial cross sections have a small offset in energy for better comparability of the error bars.

tion channels. These interactions are induced by proton or alpha emission from the giant resonance of the ^{16}O projectile. With higher energies the virtual-photon spectra become harder and the excitation of a delta resonance becomes more likely. The excitation of a delta resonance within the projectile nucleus can lead to an intranuclear cascade and can cause a more complete destruction of the projectile nucleus. That is the reason why the $\Delta Z\geq 3$ channel exceeds the $\Delta Z=2$ channel at 200 GeV/nucleon. This fact was also observed for ^{32}S data at 200 GeV/nucleon [10].

C. Cross sections for light targets

The cross sections of the three light targets CH_2, CR-39, and C were used for the determination of the hydrogen-target cross sections. The energy dependence of the total charge-changing cross sections together with cross-section data of Webber, Kish, and Schrier [42,43] are shown in Fig. 6. It turns out that the data of Webber, Kish, and Schrier match our data at 2 GeV/nucleon

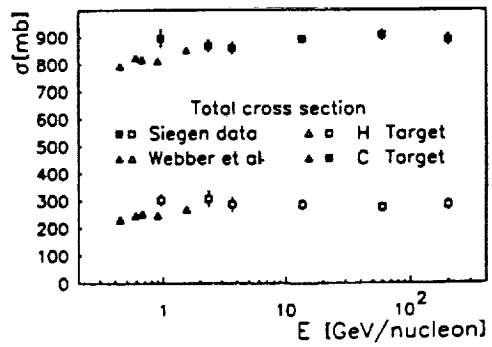

FIG. 6. Total charge-changing cross sections for ^{16}O for H and C targets. The squares (open for the H target, solid for the C target) represent our data, while the triangles give the data measured by Webber, Kish, and Schrier [42,43] (open triangle for the H target, solid triangle for the C target).

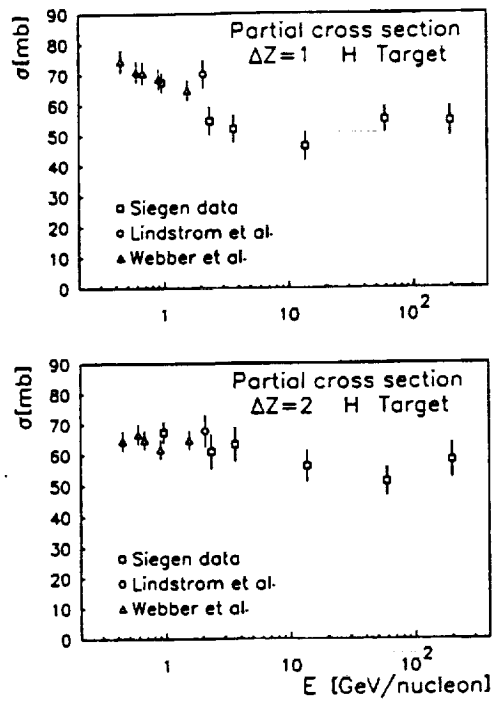

FIG. 7. Energy dependence of partial cross sections for $\Delta Z=1$ (top) and $\Delta Z=2$ (bottom) reaction of ^{16}O with hydrogen. Data from Webber, Kish, and Schrier [42,43] (open triangles) and Lindstrom *et al.* [23] (open circles) are also included.

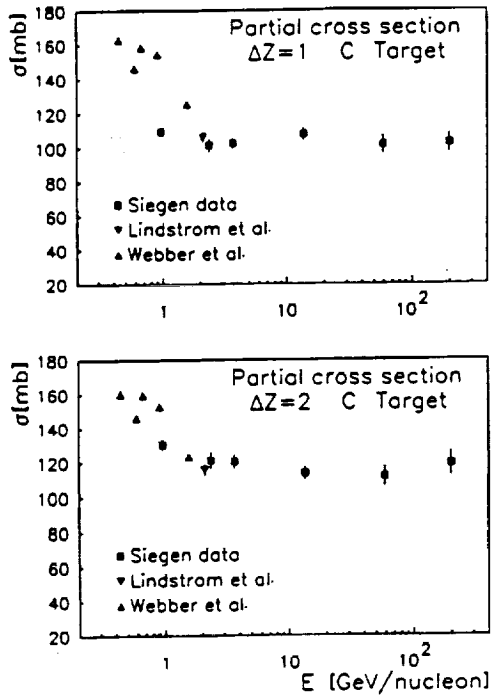

FIG. 8. Energy dependence of partial cross sections $\Delta Z=1$ (top) and $\Delta Z=2$ (bottom) for reaction of ^{16}O with carbon. Data from Webber, Kish, and Schrier [42,43] (triangles) and Lindstrom *et al.* [23] (inverted triangles) are also included.

quite well, whereas at 1 GeV/nucleon their cross sections are about 10% smaller. Figure 7 gives the partial cross section for hydrogen. It shows a decrease of the cross section for $\Delta Z=1$ between 1 and 13.5 GeV/nucleon. For $\Delta Z=2$ the observed decrease is less strong. A decrease of these partial cross sections of this strength cannot be reproduced completely with intranuclear cascade calculations [44]. Further detailed studies of this effect are necessary.

Our partial cross sections for the carbon target in comparison to other data are shown in Fig. 8. The partial cross sections for $\Delta Z=1$ and 2 are constant between 2 and 200 GeV/nucleon. In contradiction to the data of Webber, Kish, and Schrier, we only observe a slight decrease from 1 to 2 GeV/nucleon. Our data point at 2.3 GeV/nucleon is consistent with the data point of Lindstrom *et al.* at 2.1 GeV/nucleon [23]. A surprising point is that for low energies the two partial cross sections $\Delta Z=1$ and 2 for the C target of Webber, Kish, and Schrier [43] show nearly no odd/even effect which is present at higher energies.

The fact that the partial hydrogen target cross sections are smaller at energies of some GeV/nucleon than expected implies a change of parameters for astrophysical models for propagation of cosmic-ray heavy ions from the sources to the Earth. These calculations relate measured nuclear abundances near the Earth to source compositions. The thickness of penetrated matter and the probabilities of the nuclei escaping our Galaxy are obtained in these calculations. A reduced partial fragmentation cross section $\Delta Z=1$ (^{16}O$\rightarrow$N), which must be put into these calculations to reproduce the experimental data, e.g., for the measured N/O ratio, affects the escape probabilities [45].

III. CONCLUSION

Fragmentation cross sections for ^{16}O were measured for a set of targets in the energy range from 0.9 to 200 GeV/nucleon. The rise of the total charge-changing cross sections with energy, especially for heavy targets caused by the ED effect, was observed. The contribution of the ED process was calculated using virtual-photon spectra and photonuclear data. Subtracting this ED contribution from the measured total cross sections, we obtained the pure nuclear component of the cross sections. The total nuclear cross sections for all targets show no energy dependence, as is expected by the concept of limiting fragmentation. Fit procedures enabled us to separate nuclear and ED components also for the partial cross sections. The partial nuclear cross sections for heavier targets are almost energy independent and agree quite well with other data. The partial ED cross sections show that with high energies (> 100 GeV/nucleon) the ED process cannot lead to the emission of nucleons and α particles only, but can result in a much more complete destruction of the projectile nucleus. The data for the H target may influence the output of astrophysical model calculations.

ACKNOWLEDGMENTS

We are thankful to the staffs of Brookhaven and Dubna laboratories. This work was funded by the German Federal Ministry for Research and Technology (BMFT) under Contract No. 06 SI 146.

1466

[1] H. H. Heckman and P. J. Lindstrom, Phys. Rev. Lett. **37**, 56 (1976).
[2] D. L. Olson, B. L. Berman, D. E. Greiner, H. H. Heckman, P. J. Lindstrom, G. D. Westfall, and H. J. Crawford, Phys. Rev. C **24**, 1529 (1981).
[3] N. Ardito *et al.*, Europhys. Lett. **6**, 131 (1988).
[4] P. B. Price, R. Guoxiao, and W. T. Williams, Phys. Rev. Lett. **61**, 2193 (1989).
[5] G. Singh, K. Sengupta, and P. L. Jain, Phys. Rev. C **41**, 999 (1990).
[6] J. Barette *et al.*, Phys. Rev. C **41**, 1512 (1990).
[7] G. Baroni *et al.*, Nucl. Phys. **A531**, 691 (1991).
[8] S. Y. Bahk *et al.*, Phys. Rev. C **43**, 1410 (1991).
[9] C. Brechtmann and W. Heinrich, Z. Phys. A **330**, 407 (1988).
[10] C. Brechtmann and W. Heinrich, Z. Phys. A **331**, 463 (1988).
[11] C. Brechtmann and W. Heinrich, Phys. Rev. C **39**, 2222 (1989).
[12] W. Heinrich and C. Brechtmann, Mod. Phys. Lett. A **4**, 1879 (1989).
[13] W. Heinrich, C. Brechtmann, S. E. Hirzebruch, E. Winkel, K. D. Tolstov, and A. D. Kovalenko, in *Relativistic Nuclear Physics and Quantum Chromodynamics*, edited by A. M. Baldin, V. V. Burov, and L. P. Kaptari (World Scientific, Singapore, 1991), p. 509.
[14] J. C. Hill, F. K. Wohn, J. A. Winger, and A. R. Smith, Phys. Rev. Lett. **60**, 999 (1988).
[15] J. C. Hill, F. K. Wohn, J. A. Winger, M. Khayat, K. Leininger, and A. R. Smith, Phys. Rev. C **38**, 1722 (1988).
[16] J. C. Hill, F. K. Wohn, J. A. Winger, M. Khayat, M. T. Mercier, and A. R. Smith, Phys. Rev. C **39**, 524 (1989).
[17] J. C. Hill, F. K. Wohn, and D. D. Schwellenbach, Phys. Lett. B **273**, 371 (1991).
[18] D. L. Olson, M. Baumgartner, D. E. Greiner, P. J. Lindstrom, T. J. M. Symons, R. Wada, M. L. Webb, B. L. Berman, H. J. Crawford, and J. M. Engelage, Phys. Rev. C **44**, 1862 (1991).
[19] W. Heinrich, C. Brechtmann, S. E. Hirzebruch, E. Winkel, and G. Rusch, in Proceedings of the 21st International Cosmic Ray Conference, Adelaide, 1990 (unpublished), Vol. 3, p. 436.
[20] S. E. Hirzebruch, W. Heinrich, K. D. Tolstov, and A. D. Kovalenko, in Proceedings of the 22nd International Cosmic Ray Conference, Dublin, 1991 (unpublished), Vol. 2, p. 280.
[21] C. Brechtmann and W. Heinrich, Nucl. Instrum. Methods B **29**, 675 (1988).
[22] W. Trakowski, B. Schöfer, J. Dreute, S. Sonntag, C. Brechtmann, J. Beer, H. Drechsel, and W. Heinrich, Nucl. Instrum. Methods **225**, 92 (1984).
[23] P. J. Lindstrom, D. E. Greiner, H. H. Heckman, B. Cork, and F. S. Bieser, in Proceedings of the 14th ICRC, Munich, 1975 (unpublished), p. 2315.
[24] G. D. Westfall, L. W. Wilson, P. J. Lindstrom, H. J. Crawford, D. E. Greiner, and H. H. Heckman, Phys. Rev. C **19**, 1309 (1979).
[25] S. Kox *et al.*, Phys. Rev. C **35**, 1687 (1987).
[26] W. R. Binns, T. L. Garrard, M. H. Israel, M. P. Kertzmann, J. Klarmann, E. C. Stone, and C. J. Waddington, Phys. Rev. C **36**, 1870 (1987).
[27] C. A. Bertulani and G. Baur, Nucl. Phys. **A442**, 739 (1985).
[28] C. A. Bertulani and G. Baur, Nucl. Phys. **A458**, 725 (1986).
[29] G. Baur and C. A. Bertulani, Phys. Rev. C **34**, 1654 (1986).
[30] J. S. Levinger, Phys. Rev. **84**, 43 (1951).
[31] C. F. Weizsäcker, Z. Phys. **88**, 612 (1934).
[32] E. J. Williams, Phys. Rev. **45**, 729 (1934).
[33] J. W. Norbury, Phys. Rev. C **41**, 372 (1990).
[34] J. W. Norbury, Phys. Rev. C **42**, 711 (1990).
[35] J. W. Norbury, Phys. Rev. C **42**, 2259 (1990).
[36] R. Fleischhauer and W. Scheid, Nucl. Phys. **A510**, 817 (1990).
[37] E. G. Fuller, Phys. Rep. **127**, 185 (1985).
[38] C. J. Benesh, B. C. Cook, and J. P. Vary, Phys. Rev. C **40**, 1198 (1989).
[39] W. J. Llope and P. Braun-Munziger, Phys. Rev. C **41**, 2644 (1990).
[40] W. J. Llope and P. Braun-Munziger, Phys. Rev. C **45**, 799 (1992).
[41] D. L. Olson, B. L. Berman, D. E. Greiner, H. H. Heckman, P. J. Lindstrom, and H. J. Crawford, Phys. Rev. C **28**, 1602 (1983).
[42] W. R. Webber, J. C. Kish, and D. A. Schrier, Phys. Rev. C **41**, 520 (1990).
[43] W. R. Webber, J. C. Kish, and D. A. Schrier, Phys. Rev. C **41**, 533 (1990).
[44] P. Kozma (private communication).
[45] J. P. Meyer, in Proceedings of the 19th International Cosmic Ray Conference, La Jolla, 1985 (unpublished), Vol. 9, p. 141.